

Multiple Mechanisms Quench Passive Spiral Galaxies

Amelia Fraser-McKelvie^{1,2,3*}, Michael J. I. Brown^{2,3}, Kevin Pimbblet⁴,
Tim Dolley^{2,3}, Nicolas J. Bonne⁵.

¹ School of Physics & Astronomy, University of Nottingham, University Park, Nottingham, NG7 2RD, U.K.

² School of Physics and Astronomy, Monash University, Clayton, Victoria 3800, Australia

³ Monash Centre for Astrophysics (MoCA), Monash University, Clayton, Victoria 3800, Australia

⁴ E. A. Milne Centre for Astrophysics, University of Hull, Cottingham Road, Kingston-upon-Hull, HU6 7RX, U.K.

⁵ Institute of Cosmology and Gravitation, University of Portsmouth, Dennis Sciama Building, Burnaby Road, Portsmouth PO1 3FX, U.K.

31 October 2017

ABSTRACT

We examine the properties of a sample of 35 nearby passive spiral galaxies in order to determine their dominant quenching mechanism(s). All five low mass ($M_{\star} < 1 \times 10^{10} M_{\odot}$) passive spiral galaxies are located in the rich Virgo cluster. This is in contrast to low mass spiral galaxies with star formation, which inhabit a range of environments. We postulate that cluster-scale gas stripping and heating mechanisms operating only in rich clusters are required to quench low mass passive spirals, and ram-pressure stripping and strangulation are obvious candidates.

For higher mass passive spirals, while trends are present, the story is less clear. The passive spiral bar fraction is high: $74 \pm 15\%$, compared with $36 \pm 5\%$ for a mass, redshift, and T-type matched comparison sample of star forming spiral galaxies. The high mass passive spirals occur mostly, but not exclusively, in groups, and can be central or satellite galaxies. The passive spiral group fraction of $74 \pm 15\%$ is similar to that of the comparison sample of star forming galaxies at $61 \pm 7\%$. We find evidence for both quenching via internal structure and environment in our passive spiral sample, though some galaxies have evidence of neither. From this, we conclude no one mechanism is responsible for quenching star formation in passive spiral galaxies - rather, a mixture of mechanisms are required to produce the passive spiral distribution we see today.

Key words: galaxies: evolution – galaxies: general – galaxies: stellar content – galaxies: spiral

1 INTRODUCTION

In the established picture of galaxy evolution, a galaxy is likely to be quenched if it is massive (e.g. Kauffmann et al. 2003), or located in a dense environment (e.g. Peng et al. 2010). Low mass quenched galaxies are preferentially satellites (e.g. Geha et al. 2012; Davies et al. 2016), and the vast majority of quenched galaxies possess early type morphology (e.g. Strateva et al. 2001; Bell et al. 2012). This implies that the mechanism(s) responsible for quenching star formation in most galaxies also result in morphological transformation, or vice versa.

Quenching mechanisms that alter morphology include processes that strip a galaxy of its gas upon entry into a denser environment, such as galaxy harassment (Lake et al. 1998; Moore et al. 1996), galaxy-galaxy mergers (Toomre &

Toomre 1972; White & Rees 1978; Kormendy & Ho 2013), and tidal stripping. There do exist environmental mechanisms that can quench a galaxy without impacting its morphology, however. Ram-pressure stripping (Gunn & Gott 1972; van Gorkom 2004; Bekki 2009) occurs in large galaxy clusters and strips the halo and disk of cold gas used as fuel for star formation without destroying the disk (e.g. Weinmann et al. 2006). Strangulation also acts to cut off the gas supply from the galaxy’s sub-halo, causing star formation to cease when its gas reservoir is consumed (e.g. Larson et al. 1980; Balogh et al. 2000). Mass quenching mechanisms such as AGN heating also act to cease star formation without destroying a galaxy’s disk (e.g. Tabor & Binney 1993; Fabian et al. 1994).

There exist galaxies that do not conform to the above quenching paradigm, such as massive, star forming disks (e.g. Ogle et al. 2016), and spiral galaxies that show no signs of star formation (Fraser-McKelvie et al. 2016). Passive spi-

* Amelia.Fraser-Mckelvie@nottingham.ac.uk

ral galaxies are rare but intriguing objects, as their existence asserts that morphological transformation is not always required to quench star formation. While red spiral galaxies have been discussed in the literature for over 40 years, (e.g. [van den Bergh 1976](#); [Goto et al. 2003](#); [Ishigaki et al. 2007](#); [Bamford et al. 2009](#); [Skibba et al. 2009](#); [Wolf et al. 2009](#); [Bundy et al. 2010](#); [Masters et al. 2010](#); [Rowlands et al. 2012](#)), these earlier samples often showed evidence of nebular line emission, ultraviolet (UV) light from young stellar populations, or infrared (IR) excess from warm dust (e.g. [Cortese 2012](#)). For this reason, we define spiral galaxies that are optically red as red spirals, and those spirals without any signs of star formation as passive spiral galaxies.

In [Fraser-McKelvie et al. \(2016\)](#), we presented a photometrically and spectroscopically confirmed sample of passive spiral galaxies, selected using a mid-IR colour cut to ensure quiescence. These galaxies spanned a range of stellar masses, yet were uniformly passive and contained undisturbed spiral arms. Given that the mechanism(s) that cease star formation in passive spiral galaxies must do so without disrupting spiral structure, we may question whether the traditional quenching mechanisms that often destroy internal structure are occurring within these galaxies. The alternative hypothesis is that unique quenching pathways may be invoked to quench passive spiral galaxies, and this is the topic of this paper.

Alternate quenching mechanisms that do not require high stellar mass nor dense environmental regions have been characterised in the literature: for example morphological quenching (e.g. [Martig et al. 2009](#)), or extra heating provided by the winds of dying low mass stars ([Conroy et al. 2015](#)). These mechanisms have only been described in early type galaxies, however, and it is unclear whether they are also effective at quenching disk galaxies. In low mass galaxies, supernovae winds can expel a large fraction of interstellar medium on short timescales, also quenching star formation (e.g. [Dekel & Silk 1986](#); [Yepes et al. 1997](#); [Scannapieco et al. 2008](#); [Bower et al. 2017](#)).

The role of bars in galaxy evolution and quenching is well studied (e.g. [Kormendy 1979](#); [Kormendy & Kennicutt 2004](#); [Ellison et al. 2011](#); [Cheung et al. 2013](#)). By channelling cold gas into the central regions of galaxies forcing a short lived starburst, bars are one of the most efficient redistributors of gas in the disks of galaxies (e.g. [Combes & Sanders 1981](#); [Weinberg 1985](#); [Friedli & Benz 1995](#); [Athanasoula 2002](#); [Knapen et al. 2002](#); [Masters et al. 2011](#); [Athanasoula 2013](#); [Holmes et al. 2015](#)).

Simulations show strong bars are difficult to destroy once created (e.g. [Shen & Sellwood 2004](#); [Debattista et al. 2006](#)), and are capable of driving gas into the nuclear regions of galaxies (e.g. [Shlosman et al. 1989](#); [Martinet & Friedli 1997](#); [Jogee et al. 2005](#); [Spinoso et al. 2017](#); [Khoperskov et al. 2017](#)). The resultant quenched galaxy retains its spiral structure (e.g. [Cheung et al. 2013](#); [Gavazzi et al. 2015](#)). Therefore, naturally we may suspect bars (or the mechanisms that create them) as being involved in passive spiral quenching.

Given the above quenching pathways, we wish to determine whether passive spiral galaxies have particular morphologies or environments that clearly distinguish them from other spiral galaxies, and thus identify or constrain their quenching mechanisms. To achieve this, we define a

sample of passive spiral galaxies, along with a mass, redshift (z), and T-type-matched comparison sample.

This paper is organised as follows: in Section 2 we describe the sample of passive spiral galaxies used for this work, and in Section 3, we detail the control sample of spiral galaxies used for comparison. In Section 4 we examine the quenching mechanisms responsible for the formation of passive spirals by splitting our sample into high and low mass bins. Throughout this paper we use AB magnitudes and a flat Λ CDM cosmology, with $\Omega_m = 0.3$, $\Omega_\Lambda = 0.7$ and $H_0 = 70 \text{ km s}^{-1} \text{ Mpc}^2$.

2 PASSIVE SPIRAL SAMPLE

To create our passive spiral sample, we use a similar method to [Fraser-McKelvie et al. \(2016\)](#), with some added refinements. We begin with the catalogue of [Bonne et al. \(2015\)](#), which is an all-sky sample of 13,325 local Universe galaxies drawn from the 2-Micron All-Sky Survey (2MASS) Extended Source Catalogue ([Jarrett et al. 2000](#)). This catalogue has a redshift and morphological completeness of 99% to $K = 12.59$, with the majority of morphologies (in the form of T-types) coming from the PGC catalogue ([Paturel et al. 2003](#)).

We limit our analysis to the Sloan Digital Sky Survey (SDSS) imaging regions, to aid in accurate morphological classification using a large sample of uniform imaging. We select galaxies with $-3 < \text{T-type} < 8$, which allows for the misclassification of spirals as lenticulars, and perform the mid-IR colour cut of $M_K - M_{W3} < -2.73$, where M_K and M_{W3} are the 2MASS K -band and Wide-Field Survey Explorer (WISE) $12 \mu\text{m}$ k -corrected absolute magnitudes respectively. [Fraser-McKelvie et al. \(2016\)](#) showed this mid-IR colour cut is effective at separating passive spiral galaxies from optically red galaxies suffering from dust-obscured star formation. We confirm spiral morphology by visually inspecting each passive spiral candidate using SDSS colour images. Edge on galaxies, shell galaxies, merger remnants, and elliptical and lenticular galaxies are rejected from our sample, leaving 35 bona fide spiral galaxies with passive mid-IR colour.

Our passive spiral sample spans the SDSS DR13 coverage region, and:

- $0.0024 < z < 0.033$
- $3.9 \times 10^9 M_\odot < M_\star < 8.5 \times 10^{10} M_\odot$
- $1 < \text{T-type} < 8$,

where stellar masses are sourced from the NASA Sloan Atlas¹.

We note there is no crossover between our passive spiral sample and that of the optically-identified red spirals of [Masters et al. \(2010\)](#). In an effort to produce a sample dominated by disk spirals, [Masters et al. \(2010\)](#) selected only red spirals with a small bulge size using the SDSS quantity $\text{fracdeV} < 0.5$, where fracdeV measures the fraction of the galaxy light fit by a de Vaucouleurs profile. In Figure 1 we plot a normalised probability histogram of the SDSS value

¹ www.nsatlas.org

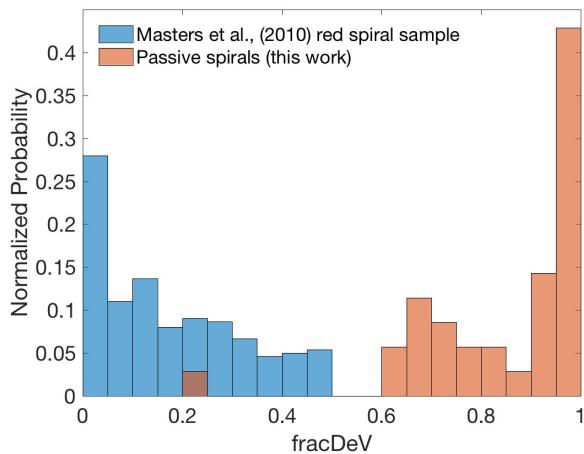


Figure 1. Comparison of the fracDeV quantity, a proxy for bulge size between the red spirals sample of [Masters et al. \(2010\)](#) in blue, and the passive spirals selected in this work (orange). Just one galaxy from our sample has $\text{fracDeV} < 0.5$, and this is NGC 4880. We expect the almost bimodal distribution in bulge size between this work and that of [Masters et al. \(2010\)](#) is the reason that our passive spiral sample is more passive.

fracDeV of both our passive spiral sample, and the [Masters et al. \(2010\)](#) red spirals. Just one galaxy in our sample has $\text{fracDeV} < 0.5$, highlighting the dichotomy between the [Masters et al. \(2010\)](#) sample and our own. We suggest that the reason our passive spiral sample is more passive than the red spirals of [Masters et al. \(2010\)](#) is simply because by making a cut in fracDeV , they excluded the most passive spiral galaxies.

3 COMPARISON SAMPLE SELECTION

In order to analyse the trends seen in our passive spiral sample, we create a control sample of spiral galaxies. As bar fraction is correlated with stellar mass (e.g. [Cameron et al. 2010](#); [Melvin et al. 2014](#)) and T-type (e.g. [Nair & Abraham 2010](#); [Martinez-Valpuesta et al. 2007](#)), we elect to match our control sample in stellar mass, T-type, and z . To create the control sample, we take all galaxies from the [Bonne et al. \(2015\)](#) catalogue, the parent catalogue of the passive spiral sample, and select the four galaxies that are closest in z and mass to each passive spiral galaxy. We impose the constraint that the T-type of the comparison galaxy must match that of the passive spiral galaxy it is being compared to. If the T-type of the passive spiral galaxy is listed as < 1 , we re-classify the galaxy, and select comparison galaxies according to the new T-type given. We note that to ensure a meaningful comparison can be made between passive and non-passive spirals, we include the restriction that a galaxy already designated as a passive spiral galaxy cannot be used as a comparison for any other passive spiral galaxy and each comparison galaxy may only be used once. We select the four galaxies nearest in mass and z range to each passive spiral galaxy with the same T-type for a sample of 140, spanning:

- $0.0027 < z < 0.043$
- $7.1 \times 10^8 M_{\odot} < M_{\star} < 9.0 \times 10^{10} M_{\odot}$,

- $1 < \text{T-type} < 8$.

We additionally require that all galaxies are within the SDSS DR13 imaging regions to ensure ease of morphological classification, and with axis ratio greater than 0.4, to enable easy feature identification. We clean the sample to remove any lenticulars or merging galaxies that have been misclassified.

In Figure 2 we provide some examples of SDSS images of the passive spiral galaxies in our sample in the left column, and the mass-matched comparison galaxies are shown in the four right columns. All galaxies not already shown in the body of this paper are included in Figure A1. We use this comparison sample to compare the trends seen in the passive spiral sample.

4 QUENCHING MECHANISMS

We search for viable quenching pathways for our sample of passive spiral galaxies by determining their mass, environmental, and internal structure properties. Given the dichotomy in galaxy properties and traditional quenching pathways present in mass-selected samples of galaxies (e.g. [Geha et al. 2012](#)), we split our analysis into low mass passive spirals in Section 4.1 and high mass in Section 4.2.

4.1 The Low Mass Regime

Environmental quenching can account for nearly all quiescent low mass galaxies at low redshift (e.g. [Bamford et al. 2009](#); [Peng et al. 2010](#); [Geha et al. 2012](#); [Kawinwanichakij et al. 2017](#)). Motivated by studies such as these, we examine the environmental properties of the low mass passive spirals in our sample.

[Wolf et al. \(2009\)](#) found that optically-red low mass spiral galaxies are rare – indeed, there are only five with $M_{\star} < 1 \times 10^{10} M_{\odot}$ in our sample. These five galaxies - NGC 4440, NGC 4277, NGC 4880, NGC 4305, and NGC 4264, are shown as postage stamp images with their four comparison galaxies in Figure 3.

As a first pass, in Figure 4 we consider the positions of the low mass passive spirals (gold stars) and their mass, z , and T-type-matched comparison galaxies (gold squares) on the sky. Immediately from their right ascension, declination, and distance listed in Table 1, we notice the low mass passive spiral galaxies are all part of the Virgo cluster. This is in line with results such as [Bamford et al. \(2009\)](#), who found that low mass spirals in the densest regions are mostly optically red. While the low mass passive spiral galaxies are all satellites, as predicted by the [Peng et al. \(2010\)](#) model, none are located in groups, and are instead all members of a rich cluster. The same is not true of the low mass comparison galaxies, which are spread across all environments. Of the comparison sample galaxies that are satellites, some show obvious star formation in their colour images (e.g. NGC 3380 and NGC 4413 in Figure 3). It seems that being a low mass spiral galaxy in a group or cluster is a necessary, but not sufficient condition for quenching. Therefore, the fact these low mass passive spiral galaxies are all in Virgo (and not just any sized group), is very significant.

There are many low mass passive satellite galaxies in groups in the [Bonne et al. \(2015\)](#) sample, but these are

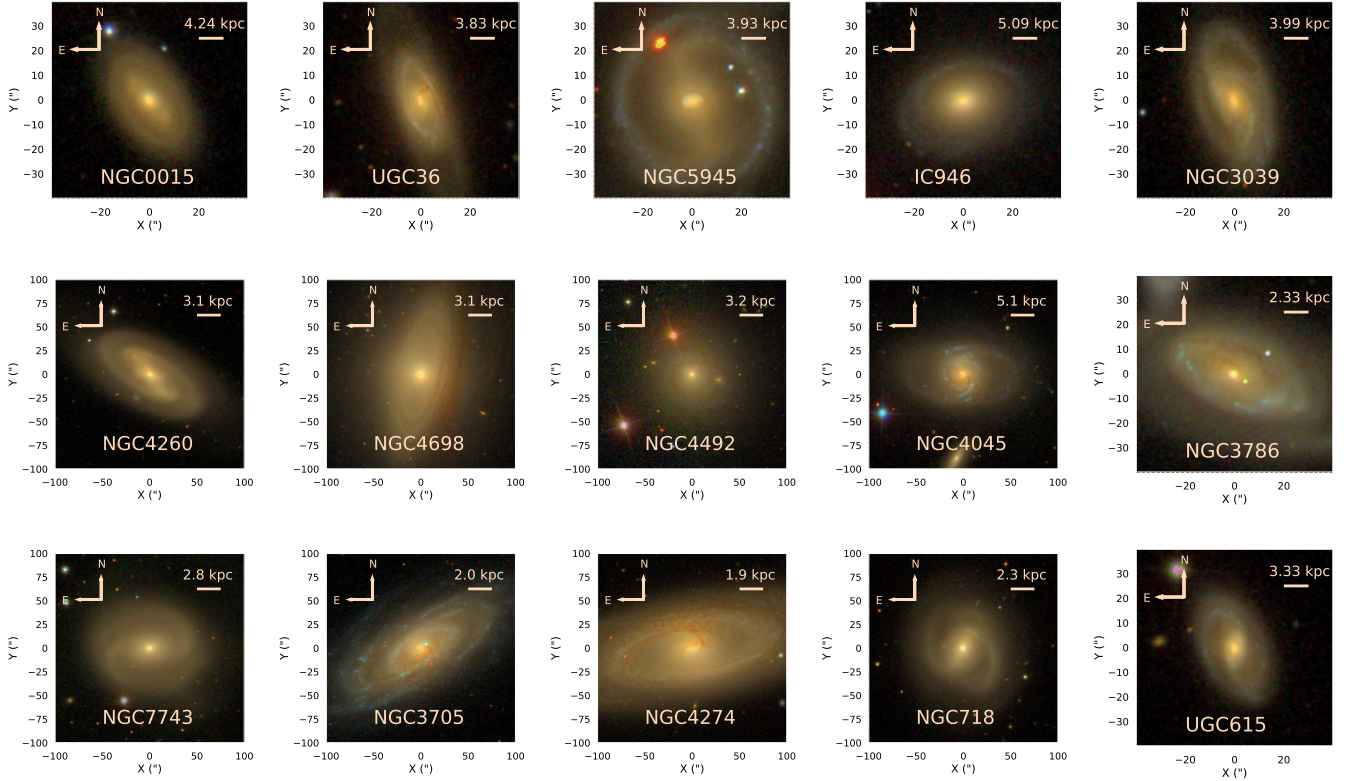


Figure 2. SDSS cutout *gri* images of some example passive spiral galaxies (left) and their four galaxies from the comparison sample closest in both z and stellar mass with the same T-type in the right four columns. While some of the galaxies in the comparison sample are red (a consequence of matching by T-type), the comparison galaxies generally show evidence for star formation including blue stellar populations and dust lanes.

mostly T-type<1 galaxies without discernible spiral structure. The obvious inference is that upon entering a group, spiral galaxies that have their star formation quenched via environmental processes will also transform their morphology from late to early type. Given the only place we have found low mass passive spirals is within the rich cluster environment, we question whether the quenching mechanism that preserves spiral morphology occurs exclusively in galaxy clusters. Alternatively, gas stripping in rich clusters may occur so quickly that we observe passive spirals before their morphology is transformed. Ram-pressure stripping has been shown in simulations to act on timescales as short as ~ 2 Gyr (Fillingham et al. 2015), for low mass galaxies, and could certainly explain our results. Either way, we speculate that the only way a spiral can avoid the violent group processes that transform its morphology is by instead entering a cluster. Cluster-specific processes such as ram-pressure stripping or strangulation can then act to strip gas gently and quench the galaxy whilst preserving its morphology.

We note here that a significant portion of our nearby galaxies are located within the Virgo cluster. All of our low mass passive spirals and 5/20 of their comparison sample counterparts are located within Virgo. We also note that we have a small sample size. We therefore determine that the chance that five galaxies are randomly located in Virgo given that 25% of low mass comparison galaxies are within Virgo to be 0.1% by the binomial theorem. From this we determine

there is only a small chance that the passive spirals may be located in Virgo by random chance.

From the above analysis, we may infer that cluster-scale gas stripping mechanisms such as ram-pressure stripping and/or strangulation may be the mechanism(s) responsible for ceasing star formation in low mass ($M_{\star} < 1 \times 10^{10} M_{\odot}$) passive spiral galaxies.

4.2 Higher Mass Passive Spirals

If prior literature on red spiral galaxies are a guide, it is unlikely higher mass ($M_{\star} > 1 \times 10^{10} M_{\odot}$) passive spiral galaxies will occupy specific environments or display unique morphologies. Previous samples of red spiral galaxies defined by optical colour selection criteria place red spirals in denser regions on average than their more star forming counterparts (e.g. Bamford et al. 2009; Masters et al. 2010), and are more likely to be satellites (Skibba et al. 2009), but with considerable spread among these trends. Optically red spirals have been found at all environmental densities, and indeed we see a range of environments listed in Table 1.

To quantify this, we match the passive spiral and comparison sample to the groups catalogue of Tully (2015), which is an all-sky groups catalogue using the 2MASS Redshift Survey as an input catalogue. While the fraction of passive spiral galaxies in groups (defined as two or more members) is high at $74 \pm 15\%$, it is comparable to the control sample of spiral galaxies with $61 \pm 7\%$. The fraction of brightest group galaxies (BGGs) and fraction of galaxies

Table 1. Passive spiral galaxies in our sample and their properties. A horizontal line separates the five galaxies in the low mass subsample discussed in Section 4.1 from the higher mass passive spiral galaxies in Section 4.2.

Name	RA (J2000)	Dec (J2000)	z^1	D ² (Mpc)	Stellar Mass ³ (M_{\odot})	T-type ⁴	N ⁵ _{group}	Galaxy ⁵ Environment	Bar? ⁶	Ansa Bar? ⁶
NGC 4440	186.9732	12.2932	0.0024	25.69	3.89×10^9	1	197	Satellite	yes	yes
NGC 4277	185.0154	5.3414	0.0083	27.60	5.36×10^9	1	39	Satellite	yes	no
NGC 4880	195.0439	12.4833	0.0051	25.55	6.85×10^9	1	1	Isolated ⁷	no	–
NGC 4305	185.5150	12.7408	0.0064	26.59	8.84×10^9	1	197	Satellite	no	–
NGC 4264	184.8991	5.8468	0.0084	27.61	9.28×10^9	1	39	Satellite	yes	yes
NGC 4260	184.8427	6.0988	0.0060	38.58*	1.97×10^{10}	1	39	Satellite	yes	no
NGC 2692	134.2418	52.0660	0.0126	30.03*	2.12×10^{10}	1	3	BGG	yes	yes
NGC 0357	15.8412	-6.3392	0.0078	27.22	2.13×10^{10}	1	1	Isolated	yes	yes
NGC 7743	356.0881	9.9341	0.0055	20.70*	2.27×10^{10}	1	2	BGG	yes	no
NGC 2648	130.6658	14.2855	0.0069	34.01*	2.45×10^{10}	1	1	Isolated ⁸	no	–
NGC 656	25.6135	26.1431	0.0131	48.77	2.51×10^{10}	1	1	Isolated	yes	yes
NGC 4608	190.3053	10.1558	0.0062	20.18*	2.95×10^{10}	1	197	Satellite	yes	yes
UGC 12800	357.5797	10.7574	0.0180	68.52	3.05×10^{10}	1	1	Isolated	yes	yes
NGC 4643	190.8339	1.9784	0.0044	26.44	3.22×10^{10}	1	1	Isolated	yes	yes
NGC 7563	348.9831	13.1962	0.0144	58.76*	3.28×10^{10}	1	7	BGG	yes	yes
NGC 2878	141.4477	2.0896	0.0243	117.63	3.30×10^{10}	2	2	BGG	yes	no
NGC 109	6.5610	21.8074	0.0182	60.16*	3.34×10^{10}	1	18	Satellite	yes	yes
UGC 01271	27.2502	13.2112	0.0170	65.76	3.46×10^{10}	1	10	Satellite	yes	yes
NGC 538	21.3585	-1.5506	0.0182	66.26*	3.59×10^{10}	2	43	Satellite	yes	no
NGC 345	15.3421	-6.8843	0.0174	67.93	4.07×10^{10}	1	9	Satellite	no	–
NGC 4596	189.9831	10.1761	0.0062	26.38	4.19×10^{10}	1	197	Satellite	yes	yes
PGC 047732	203.3438	54.9491	0.0250	114.77	4.30×10^{10}	2	1	Isolated	yes	no
UGC 8484	202.4019	32.4007	0.0247	117.32	4.47×10^{10}	3	7	Satellite	yes	yes
NGC 0015	2.2603	21.6245	0.0209	122.30*	4.50×10^{10}	1	1	Isolated	yes	no
PGC 070141	344.5540	25.2209	0.0251	99.78	4.81×10^{10}	1	9	Satellite	yes	yes
UGC 06163	166.7132	23.01627	0.0214	104.45	4.94×10^{10}	1	4	BGG	no	–
NGC 3943	178.2358	20.4791	0.0220	107.65	4.95×10^{10}	2	18	Satellite	yes	yes
PGC 67858	330.4222	-2.0983	0.0269	109.82	5.07×10^{10}	3	7	Satellite	no	–
NGC 7383	342.3986	11.5564	0.0270	108.39	5.14×10^{10}	1	10	Satellite	yes	no
NGC 7389	342.5670	11.5662	0.0264	105.51	5.70×10^{10}	3	10	Satellite	yes	yes
PGC 029301	151.4473	14.3387	0.0312	148.71	6.27×10^{10}	5	6	Satellite	yes	yes
UGC 12897	0.1581	28.3845	0.0290	126.28*	7.64×10^{10}	2	6	Satellite	no	–
NGC 550	21.6773	2.0224	0.0194	92.57*	7.75×10^{10}	1	8	Satellite	no	–
NGC 2618	128.9731	0.7072	0.0134	61.05*	8.17×10^{10}	2	1	Isolated	no	–
NGC 3527	166.8258	28.5278	0.0333	107.39*	8.52×10^{10}	1	27	Satellite	yes	yes

¹ From Bonne et al. (2015)

² * denotes redshift independent distances from NED, collated by Bonne et al. (2015), otherwise these are flow-corrected distances, calculated by Bonne et al. (2015).

³ From NASA Sloan Atlas.

⁴ Compiled by Bonne et al. (2015), most of which are from Paturel et al. (2003).

⁵ Group information from Tully (2015).

⁶ From visual inspection by the authors.

⁷ Whilst listed as isolated by Tully (2015), we expect this galaxy to be within the Virgo cluster (e.g. de Vaucouleurs 1961; Eastmond & Abell 1978).

⁸ Whilst listed as isolated by Tully (2015), this galaxy has a close companion confirmed by SDSS imaging and spectroscopy.

Table 2. The environments of both the passive spiral and mass, z , and T-type-matched comparison samples as matched to the Tully (2015) catalogue. There is no significant difference in group fraction between the passive spiral and comparison samples.

	% in groups of $N \geq 2$	% BGGs	% in clusters of $N \geq 10$	% Isolated
Passive Spiral Sample	$74 \pm 15\%$ (26/35)	$14 \pm 6\%$ (5/35)	$20 \pm 8\%$ (7/35)	$26 \pm 9\%$ (9/35)
Comparison Sample	$61 \pm 7\%$ (85/140)	$20 \pm 4\%$ (28/140)	$19 \pm 4\%$ (26/140)	$39 \pm 5\%$ (55/140)

Table 3. Bar fractions in the passive spiral sample and the mass, z , and T-type-matched comparison sample. The bar fraction and ansa bar fraction of the passive spiral sample are much higher than those of the comparison sample, suggesting bars are involved in the quenching of passive spirals.

	Bar Fraction	Ansa Bar Fraction
Passive Spiral Sample	$74 \pm 15\%$ (26/35)	$69 \pm 16\%$ (18/26)
Control Sample	$36 \pm 5\%$ (51/140)	$29 \pm 8\%$ (15/51)

located in clusters (ten or more members) are comparable for both the passive spiral and comparison sample galaxies, though passive spirals are slightly less likely to be isolated ($26 \pm 9\%$ compared to $39 \pm 5\%$ for the comparison sample). The environment fractions are listed in Table 2, and the passive spiral and comparison sample group properties listed in Tables 1 and A respectively. Given the lack of environmental trends seen in the passive spiral sample when compared to the comparison sample, we turn instead to other quench-

ing mechanisms, and examine the internal structure of the galaxies in our sample.

4.2.1 Passive Spiral Bar Fractions

Bars are an important component of disk galaxies, thought to have the ability to transfer angular momentum and gas from the disk to the central regions of a galaxy (e.g. Combes & Sanders 1981; Weinberg 1985; Masters et al. 2011). The Masters et al. (2010) red spiral sample had a bar fraction

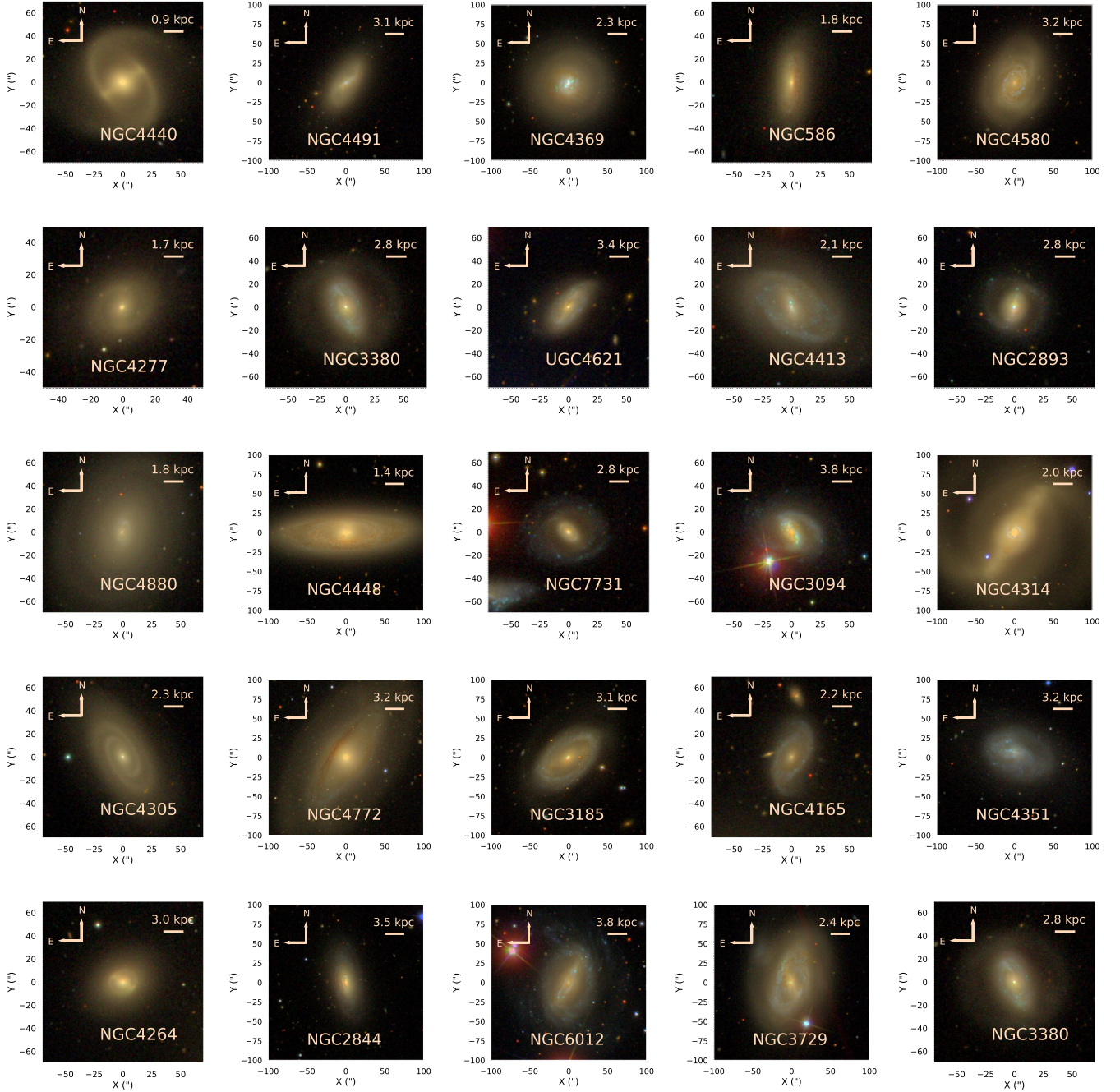


Figure 3. SDSS cutout *gri* images of the five low mass passive spiral galaxies (left) and their four galaxies from the comparison sample closest in both z and stellar mass with the same T-type in the right four columns. The five passive spirals are all located in Virgo, whilst the comparison galaxies with varying amounts of star formation are located across a range of environments.

$\sim 40\%$ higher than a similar sample of blue (or more obviously star forming) spirals. They suggest a correlation between bar instabilities and the quenching of star formation in optically red spirals. Motivated by this result, we check the bar fraction of both our passive spiral sample, and to mitigate any selection issues in bar identification, the mass, z , and T-type-matched control sample.

We visually examine the SDSS colour images of each galaxy to determine bar fraction, including both large and small bars. We note that due to the quality of the SDSS images coupled with the low redshift of the sample, small

bars within a galaxy are easily visible. The subtlety of these objects may have made them more difficult to see in older photographic plate images.

We find a significantly higher bar fraction in the passive spiral sample of $74 \pm 15\%$, compared to the comparison sample with $36 \pm 5\%$, shown in Table 3, where errors are binomial. Local Universe bar fractions have been stated to be anywhere from 20 – 30% (de Vaucouleurs et al. 1991; Masters et al. 2011), up to $\sim 50\%$ (Barazza et al. 2008; Aguerri et al. 2009). Our result is in line with the red spiral bar fraction of $67 \pm 5\%$ for the Masters et al. (2010) sample.

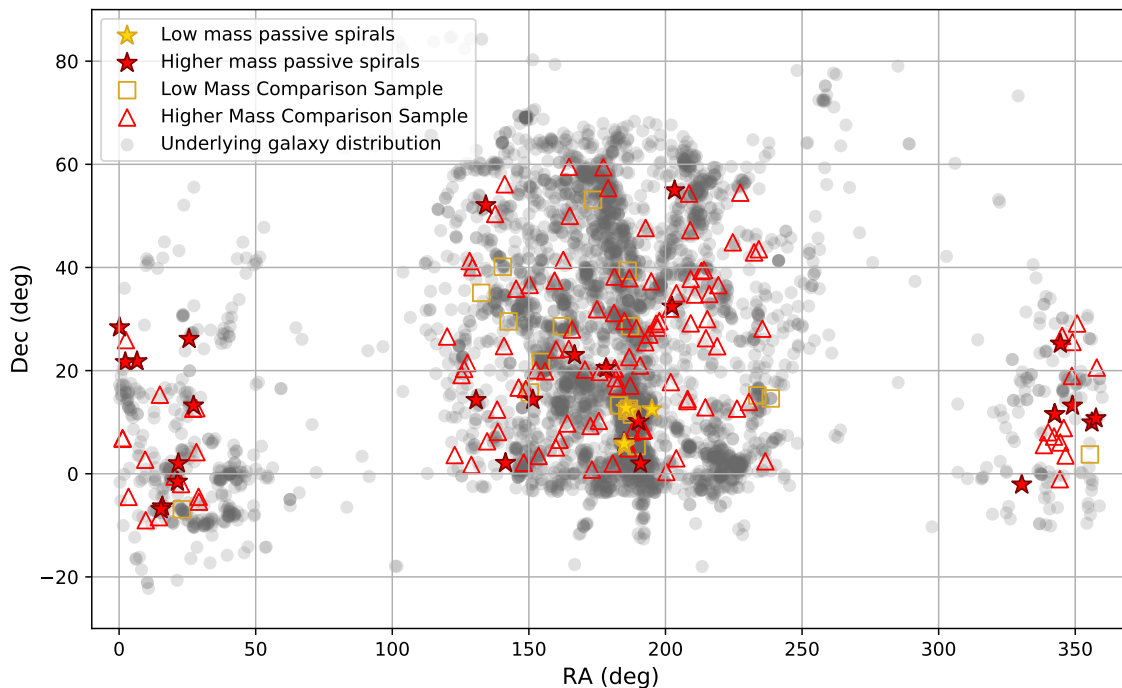


Figure 4. The position of passive spirals and comparison sample galaxies in the sky, with the underlying galaxy distribution for $z < 0.01$ from the NASA Sloan Atlas to accentuate local superstructure. Low mass passive spirals are marked as gold stars, while higher mass passive spirals are red stars. The overdensity of the Virgo cluster is clearly seen in the underlying galaxy distribution, and all low mass passive spirals lie in this region.

Ansa bars are bars that terminate with two distinct enhancements of light at either end of the bar (or a ‘handle’, e.g. [Martinez-Valpuesta et al. 2008](#)), a good example of which is shown by NGC 4440 in Figure 3. The origin of ansae is unknown, but it is thought to be related to the growth of galactic bars, with ansae appearing in simulations only after a few Gyr of evolution (e.g. [Martinez-Valpuesta et al. 2006](#)). Ansa bars are prevalent in Sa spirals, but almost non-existent in later types ([Martinez-Valpuesta et al. 2007](#)). Interestingly, the ansa bar fraction of the passive spiral sample is much higher than the comparison sample ($69 \pm 16\%$ of all barred spirals in the sample, compared to $29 \pm 8\%$), despite being matched in T-type. Bars (and ansa bars in particular) are far more common in passive spiral galaxies than comparable star forming spiral galaxies. However, whether these bars are responsible for, or a effect of, quenching is unclear.

4.2.2 Other Quenching Mechanisms

From the previous sections, one could paint a picture of quenching being a consequence of bars and environment in combination, perhaps with unbarred galaxies being satellites while barred galaxies are brightest group galaxies and isolated galaxies. This is inconsistent with the data however, as passive spiral galaxies without bars and with stellar masses of $\sim 5 \times 10^{10} M_{\odot}$ can be brightest group galaxies (UGC

6163), satellite galaxies (PGC 070141) and isolated galaxies (NGC 2618).

The one unbarred, truly isolated galaxy in our passive spiral sample, NGC 2618, has a stellar mass of $8.2 \times 10^{10} M_{\odot}$. This implies a halo mass of $\sim 10^{13} M_{\odot}$ ([Hopkins et al. 2014](#)), at which star formation is largely truncated and consistent with virial shock heating (e.g. [Dekel & Birnboim 2006](#); [Dolley et al. 2014](#)). While by definition we can invoke mass quenching to explain the most massive passive spiral galaxies, it provides few, if any, insights into the underlying astrophysics. Furthermore, all of our massive passive spiral galaxies are matched to star forming control galaxies with comparable stellar masses, so mass quenching is not deterministic (at least for our mass range).

Combining mass quenching with another mechanism is not particularly satisfying either, given passive spiral galaxies with masses in the $1 \times 10^{10} - 8.5 \times 10^{10} M_{\odot}$ range include galaxies with and without bars, isolated galaxies, and group members. Only passive spiral galaxies with masses below $1 \times 10^{10} M_{\odot}$, which all reside in Virgo, show evidence of all being quenched by the same cluster-specific mechanism. For now, we conclude that the mechanism(s) that quench the most massive passive spiral galaxies remain a puzzle.

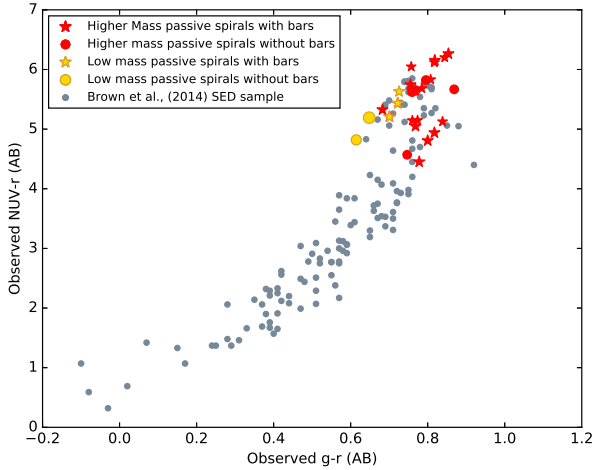


Figure 5. Optical/NUV colour colour diagram of the passive spiral sample in order to determine whether we can see evidence of particular quenching mechanisms showing up in their stellar populations. Photometry for the passive spirals is taken from matched aperture photometry of NASA Sloan Atlas images, and the underlying galaxy population from Brown et al. (2014). The low mass passive spirals are mostly bluer in $g - r$ colour than the higher mass sample, indicating either younger stellar populations, or lower metallicity (or both).

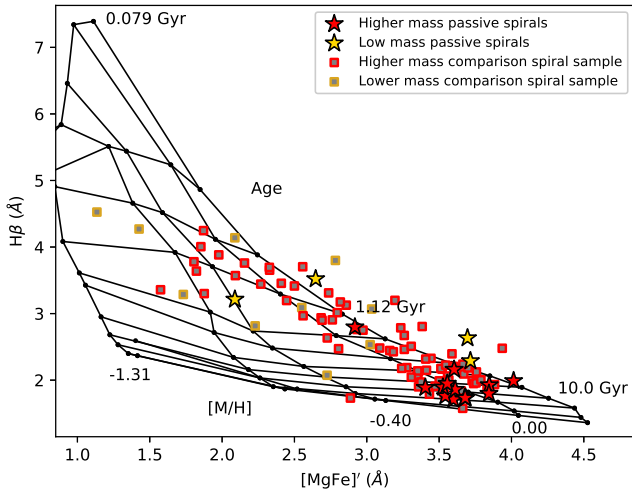


Figure 6. Spectroscopic index-index diagram for passive spiral galaxies and the mass, z , and T-type matched comparison sample using the Lick indices $H\beta$ and $[MgFe]'$ measured with SDSS-II $3''$ fibre spectroscopy of galaxy nuclei. The single stellar population model predictions of Vazdekis et al. (2010) are plotted as black lines for comparison. Of the passive spirals that have SDSS Lick index measurements, all but one of the higher mass galaxies have similar metallicities and ages, while lower mass galaxies have a broad spread of ages and metallicities. The lower mass passive spirals have on average, younger stellar populations than the high mass passive spirals. Given the lower mass passive spirals are located in a rich cluster, we may speculate that they have fallen into the cluster relatively recently.

5 STELLAR AGE AND METALLICITY DIFFERENCES BETWEEN LOW AND HIGH MASS PASSIVE SPIRALS

Given that low mass passive spiral galaxies appear to be quenched by cluster-scale environmental processes and higher mass through a combination of mechanisms, we investigate whether evidence of the quenching mechanism shows up in a galaxy’s stellar population. We examine both the integrated colours and the central stellar age and metallicity derived from $H\beta$ and $[MgFe]'$ Lick indices of the passive spiral sample.

Figure 5 is an optical and UV colour-colour diagram, with passive spiral photometry remeasured using matched-aperture photometry of archival NASA Sloan Atlas images. We ensure that any foreground features are masked in this process. The SED sample of Brown et al. (2014) with reliable multi-band photometry is also shown to illustrate the general shape of the galaxy distribution in this colour space. High mass barred and unbarred passive spirals are systematically redder in $g - r$ colour than their low mass counterparts. Given the well-known age-metallicity degeneracy (e.g. Tremonti et al. 2004), this suggests either a younger or more metal poor stellar population in low mass passive spiral galaxies.

In an attempt to separate out the effects of stellar age and metallicity, we also present an index-index diagram of both the passive spiral sample and the comparison sample in Figure 6. $H\beta$ and $[MgFe]'$ are Lick indices sourced from the SDSS-II MPA-JHU Galspec catalogue (Kauffmann et al. 2003; Brinchmann et al. 2004; Tremonti et al. 2004) for both the passive spiral sample and the mass, z , and T-type-matched comparison sample, which provides emission line-subtracted line index measurements using the Lick IDS system for a large portion of the SDSS DR7 spectroscopic sample. Here we define

$$[MgFe]' = \sqrt{Mgb (0.72 \times Fe5270 + 0.28 \times Fe5335)},$$

as in González (1993) and Thomas et al. (2003). We use these particular indices as $H\beta$ is a good indicator of recent star formation, and $[MgFe]'$ of metallicity. We note that these indices will be measured for the nuclear regions only, as they are derived from fibre spectra. To convert the index measurements to estimates of stellar age and metallicity, on Figure 6 we overlay the single stellar population model predictions of Vazdekis et al. (2010) using Padova 2000 isochrones and a Chabrier (2003) initial mass function. We see that all but one of the high mass passive spiral galaxies with measurements in the Galspec catalogue are clustered around a similarly old stellar age and approximately Solar metallicity. This is distinct from the mass-matched comparison galaxies, whose bulges span a range of stellar ages and metallicities. These galaxies are perhaps similar to comparably massive early type galaxies.

In contrast, the four low mass passive spirals are spread across a range of metallicities and stellar ages. The low mass passive spirals have younger stellar ages than all but one of the higher mass galaxies, and while one is more metal poor than the higher mass spirals, the other three are more metal rich. From their comparatively young stellar ages, we postulate that the low mass passive spirals have fallen into Virgo and quenched relatively recently, within the past ~ 1 -

2 Gyr. The low mass comparison sample are also spread throughout stellar age and metallicity space.

The tight clustering of the higher mass passive spirals around a common age and metallicity is perhaps surprising, given their lack of coherent quenching model. We suspect the similarly old bulge stellar ages and rich metallicities mean these galaxies quenched a long time ago, and any signature of quenching is no longer visible.

6 SUMMARY & CONCLUSIONS

We investigate what quenched star formation in passive spiral galaxies, using a sample of 35 $z < 0.033$ passive spiral galaxies and a comparison sample matched in mass, z , and T-Type.

All five low mass ($M_* < 1 \times 10^{10} M_\odot$) passive spiral galaxies in our sample are members of the Virgo cluster, and thus environment driven quenching is the most likely explanation for these galaxies. A large spread in both $[\text{MgFe}]'$ and $H\beta$ Lick indices implies a range of central metallicities and stellar ages, though the oldest of the low mass passive spirals is younger than all but one of the high mass passive spiral sample. Given the implied ages and metallicities from the Vazdekis et al. (2010) models and the similar environments of the low mass passive spiral sample, we suspect these galaxies have fallen into the Virgo cluster and quenched more recently than their higher mass passive spiral counterparts. Ram-pressure stripping and/or strangulation may be the relevant quenching mechanisms.

The bar fraction of passive spiral galaxies is high: $74 \pm 15\%$, compared to $36 \pm 5\%$ for a mass, z , and T-type-matched comparison sample of spirals. The bars of passive spiral galaxies feature ansae $69 \pm 16\%$ of the time, much more frequently than the comparison sample at $29 \pm 8\%$. From this we conclude that bars or the mechanism(s) responsible for creating them may also be quenching star formation in passive spirals. This is consistent with a bar quenching scenario, where gas is funnelled via a bar to the central regions of the galaxy, promoting pseudobulge growth, and inducing a starburst, followed by eventual quenching (e.g. Friedli & Benz 1995; Knapen et al. 2002; Jogee et al. 2005).

Higher mass passive spiral galaxies are amongst the oldest and most metal rich spiral galaxies. While many high mass passive galaxies have bars and all low mass passive spiral galaxies are Virgo satellite galaxies, a simple combination of bars and environment driven quenching does not explain passive spiral galaxies. Passive spiral galaxies without bars can be brightest group galaxies (e.g. UGC 6163), satellite galaxies (e.g. NGC 345), be interacting (e.g. NGC 2648) or isolated galaxies (e.g. NGC 2618). We thus conclude no one mechanism is responsible for quenching all passive spiral galaxies in our sample. Bars (and ansa bars) seem heavily involved for many galaxies, and environment driven quenching (perhaps ram-pressure stripping or harassment) best explains the lowest mass passive spiral galaxies.

While future studies with larger sample sizes will be able to address this question in a more statistical way, large-scale galaxy integral field spectroscopic surveys may also be employed to determine stellar populations and metallicities across an entire galaxy. Surveys such as Mapping Nearby Galaxies at APO (MaNGA; Bundy et al. 2015) and

the Sydney-AAO Multi-object Integral field Spectrograph galaxy survey (SAMI; Croom et al. 2012) will provide insight into the star formation and quenching history of low and high mass passive spiral galaxies, in turn, confirming the relevant quenching mechanisms and timescales.

ACKNOWLEDGEMENTS

We wish to thank the anonymous referee for their insightful comments that improved the quality of this manuscript. AFM acknowledges the support of an Australian Postgraduate Award and a Monash Graduate Education Postgraduate Publications Award. Funding for the SDSS III has been provided by the Alfred P. Sloan Foundation, the U.S. Department of Energy Office of Science, and the Participating Institutions. This publication makes use of data products from the Wide-field Infrared Survey Explorer, which is a joint project of the University of California, Los Angeles, and the Jet Propulsion Laboratory/California Institute of Technology, funded by the National Aeronautics and Space Administration. This publication makes use of data products from the Wide-field Infrared Survey Explorer, which is a joint project of the University of California, Los Angeles, and the Jet Propulsion Laboratory/California Institute of Technology, funded by the National Aeronautics and Space Administration. This publication makes use of data products from the Two Micron All Sky Survey, which is a joint project of the University of Massachusetts and the Infrared Processing and Analysis Center/California Institute of Technology, funded by the National Aeronautics and Space Administration and the National Science Foundation.

APPENDIX A: PASSIVE SPIRAL COMPARISON SAMPLE PROPERTIES AND HIGHER MASS SAMPLE IMAGES

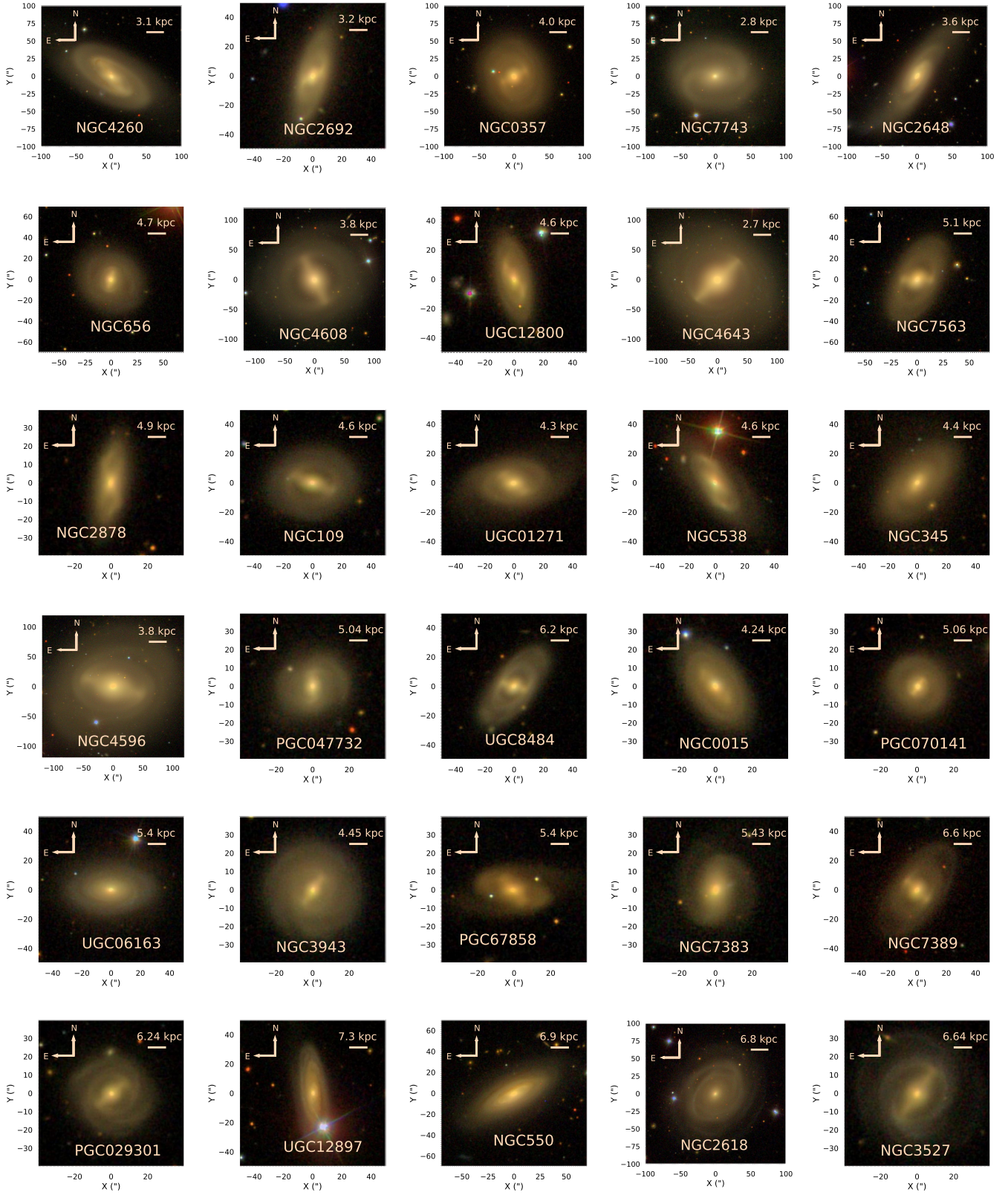


Figure A1. SDSS cutout *gri* images of the thirty galaxies in the higher mass passive spiral sample.

Table A1: The mass, z , and T-type-matched comparison sample of all spiral galaxies and their properties. The left most column denotes the passive spiral galaxy, followed by its four comparisons matched most closely in mass, z , and T-type from the sample of [Bonne et al. \(2015\)](#). The horizontal line separates the five low mass passive spiral galaxies and their comparison galaxies from their higher-mass counterparts.

Passive Spiral	Comparison Galaxy	RA (J2000)	Dec (J2000)	z^1	D ² (Mpc)	Mass ³ (M_{\odot})	T-type ⁴	N _{group} ⁵	Galaxy ⁵ Environment	Bar? ⁶	Ansa ⁶ Bar?
NGC 4440	PGC 41376	187.7381	11.4836	0.0060	25.63	7.12×10^8	1	197	satellite	yes	no
	PGC 40396	186.1508	39.3830	0.0045	19.14	3.86×10^9	1	1	isolated	no	–
	PGC 5679	22.9035	-6.8937	0.0050	21.23	3.80×10^9	1	8	satellite	no	–
	PGC 42174	189.4517	5.3684	0.0061	17.50*	4.93×10^9	1	1	isolated	no	–
NGC 4277	PGC 32287	162.0507	28.6018	0.0079	33.90	5.86×10^9	1	5	satellite	no	–
	PGC 24829	132.5492	35.0764	0.0095	43.35*	4.92×10^9	1	1	isolated	no	–
	PGC 40705	186.6344	12.6108	0.0059	22.47*	7.10×10^8	1	197	satellite	yes	no
	PGC 26979	142.5707	29.5400	0.0077	33.20	2.93×10^9	1	1	isolated	yes	no
NGC 4880	PGC 40988	187.0643	28.6203	0.0027	11.73	6.33×10^9	1	15	satellite	no	–
	PGC 72128	355.3712	3.7400	0.0078	33.59	7.86×10^9	1	2	BGG	yes	no
	PGC 30445	155.8775	19.8650	0.0052	23.57*	1.46×10^{10}	1	11	satellite	no	–
	PGC 29009	150.3580	15.7700	0.0106	35.50*	8.36×10^9	1	1	isolated	yes	no
NGC 4305	PGC 43798	193.3716	2.1683	0.0061	43.57*	9.67×10^9	1	7	satellite	no	–
	PGC 30059	154.4107	21.6882	0.0060	27.54*	8.23×10^9	1	11	satellite	yes	no
	PGC 38885	183.0492	13.2464	0.0062	57.27*	3.28×10^9	1	9	satellite	no	–
	PGC 40306	186.0065	12.2050	0.0063	29.33*	5.02×10^9	1	197	satellite	no	–
NGC 4264	PGC 26501	140.4501	40.1512	0.0068	43.75*	5.50×10^9	1	1	isolated	no	–
	PGC 56334	238.5581	14.6012	0.0073	19.99*	7.56×10^9	1	1	isolated	yes	no
	PGC 55480	233.6350	15.1938	0.0082	22.77*	8.30×10^9	1	3	BGG	no	–
	PGC 35711	173.4556	53.1255	0.0047	22.69*	8.27×10^9	1	65	satellite	no	–
NGC 4260	PGC 43254	192.0955	8.4872	0.0060	28.24*	1.95×10^{10}	1	1	isolated	no	–
	PGC 41383	187.7489	8.0779	0.0062	26.62	1.56×10^{10}	1	197	satellite	no	–
	PGC 38031	180.6761	1.9768	0.0010	28.43*	1.98×10^{10}	1	1	isolated	no	–
	PGC 36158	174.9271	31.9094	0.0114	46.73*	1.96×10^{10}	1	2	BGG	no	–
NGC 2692	PGC 49431	208.6214	54.3307	0.0167	72.25	2.12×10^{10}	1	1	isolated	yes	no
	PGC 70348	345.8153	8.8737	0.0142	49.72*	2.01×10^{10}	1	3	satellite	no	–
	PGC 34883	170.5614	20.2085	0.0173	74.64	2.11×10^{10}	1	5	satellite	no	–
	PGC 72639	357.8615	20.5862	0.0158	46.93*	2.14×10^{10}	1	1	isolated	no	–
NGC 357	PGC 29855	153.5629	3.4661	0.0041	14.62*	2.21×10^{10}	1	3	satellite	no	–
	PGC 36907	177.2668	59.4327	0.0121	52.13	2.17×10^{10}	1	7	satellite	yes	no
	PGC 33371	165.7967	27.9725	0.0075	17.87*	1.84×10^{10}	1	2	BGG	yes	no
	PGC 54110	227.3815	54.5064	0.0122	65.03*	2.04×10^{10}	1	2	BGG	yes	yes
NGC 7743	PGC 35440	172.5311	9.2766	0.0038	19.79*	1.59×10^{10}	1	2	BGG	no	–
	PGC 39724	184.9611	29.6147	0.0036	20.67*	1.56×10^{10}	1	15	satellite	no	–
	PGC 6993	28.3054	4.1958	0.0045	19.13	1.49×10^{10}	1	1	isolated	yes	no
	PGC 3563	14.9171	15.3310	0.0164	71.59*	2.22×10^{10}	1	1	isolated	yes	no
NGC 2648	PGC 70098	344.3314	-1.0490	0.0086	36.77	2.63×10^{10}	1	1	isolated	yes	no
	PGC 49604	209.2333	29.1643	0.0101	42.86*	2.59×10^{10}	1	1	isolated	yes	yes
	PGC 28631	148.8900	16.4328	0.0152	56.68*	2.42×10^{10}	1	2	Satellite	no	–
	PGC 70118	344.5018	6.0698	0.0141	60.98	2.49×10^{10}	1	1	isolated	yes	yes
NGC 656	PGC 6982	28.2487	12.7085	0.0135	57.97*	2.33×10^{10}	1	10	satellite	no	–
	PGC 37497	179.0299	55.3907	0.0208	90.32	2.60×10^{10}	1	1	isolated	no	–
	PGC 23855	127.5105	21.4885	0.0172	58.57*	2.36×10^{10}	1	3	satellite	no	–
	PGC 55993	236.5682	2.4155	0.0140	39.97*	2.84×10^{10}	1	2	BGG	no	–

NGC 4608	PGC 43451	192.6109	25.5008	0.0047	20.99*	3.00×10^{10}	1	3	BGG	no	–
	PGC 26008	138.3983	12.4408	0.0185	82.43*	2.86×10^{10}	1	1	isolated	no	–
	PGC 31701	159.8827	5.1075	0.0301	131.54	2.84×10^{10}	1	1	isolated	no	–
UGC 12800	PGC 32472	162.5900	41.4640	0.0258	112.22	3.14×10^{10}	1	1	isolated	no	–
	PGC 29631	152.6664	20.0702	0.0154	60.16*	3.04×10^{10}	1	1	isolated	no	–
	PGC 22962	122.8462	3.6331	0.0153	66.11	2.95×10^{10}	1	1	isolated	yes	no
	PGC 35594	173.0900	0.8040	0.0230	99.85	3.04×10^{10}	1	3	BGG	no	–
NGC 4643	PGC 27926	146.2379	16.7074	0.0226	97.96	3.07×10^{10}	1	1	isolated	yes	yes
	PGC 43074	191.5646	8.3484	0.0243	100.43*	3.73×10^{10}	1	1	isolated	yes	yes
	PGC 45757	197.7571	29.5783	0.0265	113.35*	3.68×10^{10}	1	2	satellite	yes	no
	PGC 45542	197.1137	28.3206	0.0242	104.97	2.68×10^{10}	1	136	satellite	yes	yes
NGC 7563	PGC 69449	340.0711	8.0537	0.0229	99.59	2.62×10^{10}	1	4	BGG	yes	no
	PGC 49563	209.0694	47.2356	0.0075	26.05*	3.28×10^{10}	1	1	isolated	no	–
	PGC 70455	346.4512	3.5451	0.0145	39.77*	3.47×10^{10}	1	3	BGG	no	–
NGC 2878	PGC 49598	209.2126	37.797	0.0120	51.59	2.30×10^{10}	1	9	satellite	yes	yes
	PGC 7322	29.2408	-5.4029	0.0149	64.19	3.45×10^{10}	1	1	isolated	yes	yes
	PGC 38288	181.3663	20.3088	0.0271	117.99	3.29×10^{10}	2	30	satellite	no	–
	PGC 38338	181.4588	20.4770	0.0252	109.54	3.29×10^{10}	2	30	satellite	no	–
NGC 109	PGC 26606	140.8979	24.7616	0.0275	109.38*	4.25×10^{10}	2	4	BGG	no	–
	PGC 26665	141.1621	56.1296	0.0264	114.88	2.45×10^{10}	2	1	isolated	yes	yes
	PGC 52261	219.3423	36.5678	0.0159	50.71*	3.38×10^{10}	1	7	satellite	yes	no
	PGC 25225	134.7103	6.2931	0.0153	65.80	3.41×10^{10}	1	1	isolated	yes	no
	PGC 6633	27.1378	12.6138	0.0165	71.28	3.52×10^{10}	1	10	satellite	yes	no
UGC 1271	PGC 70819	348.7644	18.9734	0.0151	64.94	3.26×10^{10}	1	4	satellite	no	–
	PGC 23630	126.3003	20.3348	0.0168	70.20*	2.80×10^{10}	1	21	satellite	yes	no
	PGC 50986	214.0995	39.5023	0.0212	92.02	3.67×10^{10}	1	1	isolated	yes	yes
NGC 538	PGC 24230	129.3608	40.0355	0.0253	109.84	3.63×10^{10}	1	4	satellite	no	–
	PGC 46633	200.3463	0.3426	0.0212	63.84*	3.17×10^{10}	1	1	isolated	no	–
	PGC 44557	194.7871	37.3103	0.0177	76.48	3.60×10^{10}	2	2	satellite	no	–
	PGC 38634	182.3871	17.0142	0.0251	109.08	3.57×10^{10}	2	4	satellite	yes	no
NGC 345	PGC 33040	164.6870	59.5107	0.0230	101.42*	3.56×10^{10}	2	1	isolated	no	–
	PGC 24152	128.9521	1.7217	0.0161	53.20*	2.91×10^{10}	2	3	BGG	no	–
	PGC 4906	20.3193	-0.5445	0.0157	67.85	5.07×10^{10}	1	1	isolated	yes	yes
NGC 4596	PGC 47180	201.9456	17.7789	0.0245	106.49	4.07×10^{10}	1	1	isolated	yes	no
	PGC 23441	125.3526	19.1477	0.0284	126.28*	4.07×10^{10}	1	1	isolated	no	–
	PGC 698	2.4725	25.9238	0.0132	55.18*	3.93×10^{10}	1	2	BGG	no	–
	PGC 23993	128.3242	41.2595	0.0243	105.57	4.18×10^{10}	1	8	satellite	no	–
PGC 047732	PGC 40490	186.3254	4.9251	0.0064	21.73*	3.75×10^{10}	1	39	satellite	no	–
	PGC 42743	190.7249	20.9897	0.0244	115.34*	4.22×10^{10}	1	1	isolated	yes	yes
	PGC 3486	14.5992	-8.4078	0.0128	55.19	4.46×10^{10}	1	2	BGG	no	–
	PGC 42137	189.3377	28.2081	0.0281	124.29*	4.21×10^{10}	2	2	BGG	no	–
	PGC 71258	350.6911	29.1379	0.0172	89.79*	4.26×10^{10}	2	5	satellite	no	–
	PGC 51439	216.0316	34.8589	0.0148	63.81	4.36×10^{10}	2	1	isolated	no	–
UGC 8484	PGC 28984	150.2631	36.6186	0.0240	104.24	3.93×10^{10}	2	1	isolated	no	–
	PGC 38271	181.3114	38.2355	0.0257	111.76	4.47×10^{10}	3	1	isolated	no	–
	PGC 38441	181.7644	18.5317	0.0268	107.39*	4.00×10^{10}	3	1	isolated	no	–
	PGC 53817	226.1691	12.6335	0.0307	114.35*	4.51×10^{10}	3	1	isolated	no	–
NGC 15	PGC 51283	215.3047	29.9936	0.0325	123.30*	4.43×10^{10}	3	1	isolated	no	–
	PGC 366	1.3079	6.7720	0.0189	94.16*	4.21×10^{10}	1	3	satellite	no	–
	PGC 55243	232.4375	42.9187	0.0194	59.56*	4.59×10^{10}	1	5	BGG	yes	no

	PGC 49244	208.0347	14.1163	0.0253	91.88*	4.53×10^{10}	1	5	satellite	no	–
	PGC 28452	148.1235	2.1544	0.0197	63.54*	4.30×10^{10}	1	1	isolated	no	–
PGC 070141	PGC 36436	175.8523	19.7498	0.0231	100.09	5.07×10^{10}	1	61	satellite	no	–
	PGC 69780	342.2421	7.2190	0.0226	98.01	4.87×10^{10}	1	1	isolated	yes	no
	PGC 33012	164.6050	24.2264	0.0241	107.39*	4.77×10^{10}	1	2	BGG	no	–
	PGC 40768	186.7311	37.9089	0.0247	107.19	4.70×10^{10}	1	1	isolated	yes	yes
UGC 6163	PGC 44144	194.1160	26.9875	0.0240	104.27	5.16×10^{10}	1	136	satellite	yes	no
	PGC 50042	210.7543	34.7579	0.0145	63.04*	4.95×10^{10}	1	6	satellite	no	–
	PGC 40783	186.7478	22.6395	0.0254	110.75	4.97×10^{10}	1	1	isolated	yes	yes
	PGC 47953	203.9511	2.9989	0.0243	105.44	5.10×10^{10}	1	4	satellite	no	–
NGC 3943	PGC 33126	164.9711	50.0153	0.0276	120.22	4.97×10^{10}	2	4	satellite	yes	no
	PGC 45358	196.5720	29.0631	0.0260	110.37*	5.18×10^{10}	2	136	satellite	no	–
	PGC 55601	234.1757	43.5394	0.0198	85.74	4.88×10^{10}	2	7	satellite	yes	no
	PGC 50750	213.1589	39.3102	0.0271	117.96	5.25×10^{10}	2	1	isolated	no	–
PGC 067858	PGC 27666	145.3192	35.8822	0.0251	103.41*	5.16×10^{10}	3	5	BGG	no	–
	PGC 70877	349.0029	25.5567	0.0251	109.19	4.72×10^{10}	3	9	satellite	no	–
	PGC 7259	29.0908	-4.4676	0.0161	64.43*	5.05×10^{10}	3	1	isolated	no	–
	PGC 51108	214.6165	12.8830	0.0271	119.32*	4.98×10^{10}	3	1	isolated	yes	no
NGC 7383	PGC 22445	120.0874	26.6135	0.0284	120.31*	5.15×10^{10}	1	4	BGG	yes	no
	PGC 40192	185.7985	6.0722	0.0267	116.05	5.20×10^{10}	1	2	BGG	yes	no
	PGC 47961	203.9583	34.9988	0.0270	117.57	5.08×10^{10}	1	16	satellite	no	–
	PGC 31572	159.4078	37.4557	0.0251	109.19	5.96×10^{10}	1	3	satellite	no	–
NGC 7389	PGC 38227	181.1808	31.1772	0.0274	119.51	5.70×10^{10}	3	2	BGG	no	–
	PGC 31729	159.9914	24.0913	0.0236	90.48*	5.66×10^{10}	3	1	isolated	no	–
	PGC 70250	345.2045	26.7409	0.0244	92.37*	5.99×10^{10}	3	9	satellite	yes	no
	PGC 37264	178.3347	20.7516	0.0234	102.41*	5.77×10^{10}	3	18	satellite	yes	no
PGC 029301	PGC 2331	9.7477	-9.0027	0.0185	80.01	6.27×10^{10}	5	2	BGG	no	–
	PGC 26059	138.6555	8.1172	0.0335	146.35	6.89×10^{10}	5	1	isolated	no	–
	PGC 43504	192.7480	47.6715	0.0313	105.40*	6.13×10^{10}	5	4	BGG	no	–
	PGC 32078	161.2155	6.5969	0.0307	90.68*	6.52×10^{10}	5	1	isolated	no	–
UGC 12897	PGC 54861	230.5327	13.9282	0.0320	140.05	7.52×10^{10}	2	1	isolated	no	–
	PGC 69172	338.5282	5.5703	0.0132	51.52*	7.13×10^{10}	2	1	isolated	no	–
	PGC 51167	214.8191	26.2986	0.0390	171.31	6.80×10^{10}	2	4	satellite	no	–
	PGC 49280	208.1112	14.4909	0.0433	190.92	6.99×10^{10}	2	3	BGG	no	–
NGC 550	PGC 5628	22.6696	-1.9944	0.0180	77.93	6.99×10^{10}	1	43	satellite	yes	no
	PGC 47131	201.8202	32.0307	0.0265	154.12*	7.82×10^{10}	1	7	satellite	yes	no
	PGC 25875	137.6652	50.3798	0.0184	79.39	6.78×10^{10}	1	3	satellite	yes	yes
	PGC 2279	9.5516	2.7286	0.0156	90.98*	8.42×10^{10}	1	16	satellite	no	–
NGC 2618	PGC 354	1.2760	6.9201	0.0184	79.25*	8.47×10^{10}	2	3	BGG	no	–
	PGC 41024	187.1235	17.0850	0.0061	20.45*	8.43×10^{10}	2	197	Satellite	no	–
	PGC 53508	224.6501	44.8836	0.0374	164.15	8.45×10^{10}	2	1	isolated	no	–
	PGC 916	3.4491	-4.4751	0.0346	151.44	7.80×10^{10}	2	1	isolated	yes	no
NGC 3527	PGC 32872	164.0645	9.7544	0.0362	158.84	8.81×10^{10}	1	17	satellite	no	–
	PGC 55817	235.4758	28.1341	0.0347	125.28*	8.77×10^{10}	1	10	satellite	yes	no
	PGC 52171	218.9405	24.7258	0.0381	167.05	8.96×10^{10}	1	2	BGG	no	–
	PGC 36348	175.5989	10.2641	0.0246	143.18*	8.40×10^{10}	1	9	satellite	no	–

¹ From [Bonne et al. \(2015\)](#)² * denotes redshift independent distances from NED, collated by [Bonne et al. \(2015\)](#), otherwise these are flow-corrected distances, calculated by [Bonne et al. \(2015\)](#).³ From NASA Sloan Atlas⁴ Compiled by [Bonne et al. \(2015\)](#), most of which are from [Paturel et al. \(2003\)](#).

⁵ Environmental properties from [Tully \(2015\)](#).

⁶ From visual inspection of SDSS images by the authors.

REFERENCES

- Aguerri J. A. L., Méndez-Abreu J., Corsini E. M., 2009, *A&A*, **495**, 491
- Athanassoula E., 2002, *ApJL*, **569**, L83
- Athanassoula E., 2013, Bars and secular evolution in disk galaxies: Theoretical input. p. 305
- Balogh M. L., Navarro J. F., Morris S. L., 2000, *ApJ*, **540**, 113
- Bamford S. P., et al., 2009, *MNRAS*, **393**, 1324
- Barazza F. D., Jogee S., Marinova I., 2008, *ApJ*, **675**, 1194
- Bekki K., 2009, *MNRAS*, **399**, 2221
- Bell E. F., et al., 2012, *ApJ*, **753**, 167
- Bonne N. J., Brown M. J. I., Jones H., Pimblett K. A., 2015, *ApJ*, **799**, 160
- Bower R. G., Schaye J., Frenk C. S., Theuns T., Schaller M., Crain R. A., McAlpine S., 2017, *MNRAS*, **465**, 32
- Brinchmann J., Charlot S., White S. D. M., Tremonti C., Kauffmann G., Heckman T., Brinkmann J., 2004, *MNRAS*, **351**, 1151
- Brown M. J. I., et al., 2014, *ApJS*, **212**, 18
- Bundy K., et al., 2010, *ApJ*, **719**, 1969
- Bundy K., et al., 2015, *ApJ*, **798**, 7
- Cameron E., et al., 2010, *MNRAS*, **409**, 346
- Chabrier G., 2003, *PASP*, **115**, 763
- Cheung E., et al., 2013, *ApJ*, **779**, 162
- Combes F., Sanders R. H., 1981, *A&A*, **96**, 164
- Conroy C., van Dokkum P. G., Kravtsov A., 2015, *ApJ*, **803**, 77
- Cortese L., 2012, *A&A*, **543**, A132
- Croom S. M., et al., 2012, *MNRAS*, **421**, 872
- Davies L. J. M., et al., 2016, *MNRAS*, **455**, 4013
- Debattista V. P., Mayer L., Carollo C. M., Moore B., Wadsley J., Quinn T., 2006, *ApJ*, **645**, 209
- Dekel A., Birnboim Y., 2006, *MNRAS*, **368**, 2
- Dekel A., Silk J., 1986, *ApJ*, **303**, 39
- Dolley T., et al., 2014, *ApJ*, **797**, 125
- Eastmond T. S., Abell G. O., 1978, *PASP*, **90**, 367
- Ellison S. L., Nair P., Patton D. R., Scudder J. M., Mendel J. T., Simard L., 2011, *MNRAS*, **416**, 2182
- Fabian A. C., Arnaud K. A., Bautz M. W., Tawara Y., 1994, *ApJL*, **436**, L63
- Fillingham S. P., Cooper M. C., Wheeler C., Garrison-Kimmel S., Boylan-Kolchin M., Bullock J. S., 2015, *MNRAS*, **454**, 2039
- Fraser-McKelvie A., Brown M. J. I., Pimblett K. A., Dolley T., Crossett J. P., Bonne N. J., 2016, *MNRAS*, **462**, L11
- Friedli D., Benz W., 1995, *A&A*, **301**, 649
- Gavazzi G., et al., 2015, *A&A*, **580**, A116
- Geha M., Blanton M. R., Yan R., Tinker J. L., 2012, *ApJ*, **757**, 85
- González J. J., 1993, PhD thesis, Thesis (PH.D.)—UNIVERSITY OF CALIFORNIA, SANTA CRUZ, 1993. Source: Dissertation Abstracts International, Volume: 54-05, Section: B, page: 2551.
- Goto T., et al., 2003, *PASJ*, **55**, 757
- Gunn J. E., Gott III J. R., 1972, *ApJ*, **176**, 1
- Holmes L., et al., 2015, *MNRAS*, **451**, 4397
- Hopkins P. F., Kereš D., Oñorbe J., Faucher-Giguère C.-A., Quataert E., Murray N., Bullock J. S., 2014, *MNRAS*, **445**, 581
- Ishigaki M., Goto T., Matsuhara H., 2007, *MNRAS*, **382**, 270
- Jarrett T. H., Chester T., Cutri R., Schneider S., Skrutskie M., Huchra J. P., 2000, *AJ*, **119**, 2498
- Jogee S., Scoville N., Kenney J. D. P., 2005, *ApJ*, **630**, 837
- Kauffmann G., et al., 2003, *MNRAS*, **341**, 54
- Kawinwanichakij L., et al., 2017, preprint, ([arXiv:1706.03780](https://arxiv.org/abs/1706.03780))
- Khoperskov S., Haywood M., Di Matteo P., Lehnert M. D., Combes F., 2017, preprint, ([arXiv:1709.03604](https://arxiv.org/abs/1709.03604))
- Knapen J. H., Pérez-Ramírez D., Laine S., 2002, *MNRAS*, **337**, 808
- Kormendy J., 1979, *ApJ*, **227**, 714
- Kormendy J., Ho L. C., 2013, *ARA&A*, **51**, 511
- Kormendy J., Kennicutt Jr. R. C., 2004, *ARA&A*, **42**, 603
- Lake G., Katz N., Moore B., 1998, *ApJ*, **495**, 152
- Larson R. B., Tinsley B. M., Caldwell C. N., 1980, *ApJ*, **237**, 692
- Martig M., Bournaud F., Teyssier R., Dekel A., 2009, *ApJ*, **707**, 250
- Martinet L., Friedli D., 1997, *A&A*, **323**, 363
- Martinez-Valpuesta I., Shlosman I., Heller C., 2006, *ApJ*, **637**, 214
- Martinez-Valpuesta I., Knapen J. H., Buta R., 2007, *AJ*, **134**, 1863
- Martinez-Valpuesta I., Knapen J. H., Buta R., 2008, in Knapen J. H., Mahoney T. J., Vazdekis A., eds, *Astronomical Society of the Pacific Conference Series Vol. 390, Pathways Through an Eclectic Universe*. p. 304
- Masters K. L., et al., 2010, *MNRAS*, **405**, 783
- Masters K. L., et al., 2011, *MNRAS*, **411**, 2026
- Melvin T., et al., 2014, *MNRAS*, **438**, 2882
- Moore B., Katz N., Lake G., Dressler A., Oemler A., 1996, *Nature*, **379**, 613
- Nair P. B., Abraham R. G., 2010, *ApJS*, **186**, 427
- Ogle P. M., Lanz L., Nader C., Helou G., 2016, *ApJ*, **817**, 109
- Paturel G., Petit C., Prugniel P., Theureau G., Rousseau J., Brouty M., Dubois P., Cambrésy L., 2003, *A&A*, **412**, 45
- Peng Y.-j., et al., 2010, *ApJ*, **721**, 193
- Rowlands K., et al., 2012, *MNRAS*, **419**, 2545
- Scannapieco C., Tissera P. B., White S. D. M., Springel V., 2008, *MNRAS*, **389**, 1137
- Shen J., Sellwood J. A., 2004, *ApJ*, **604**, 614
- Shlosman I., Frank J., Begelman M. C., 1989, *Nature*, **338**, 45
- Skibba R. A., et al., 2009, *MNRAS*, **399**, 966
- Spinoso D., Bonoli S., Dotti M., Mayer L., Madau P., Bellovary J., 2017, *MNRAS*, **465**, 3729
- Strateva I., et al., 2001, *AJ*, **122**, 1861
- Tabor G., Binney J., 1993, *MNRAS*, **263**, 323
- Thomas D., Maraston C., Bender R., 2003, *MNRAS*, **339**, 897
- Toomre A., Toomre J., 1972, *ApJ*, **178**, 623
- Tremonti C. A., et al., 2004, *ApJ*, **613**, 898
- Tully R. B., 2015, *AJ*, **149**, 171
- Vazdekis A., Sánchez-Blázquez P., Falcón-Barroso J., Cenarro A. J., Beasley M. A., Cardiel N., Gorgas J., Peletier R. F., 2010, *MNRAS*, **404**, 1639
- Weinberg M. D., 1985, *MNRAS*, **213**, 451
- Weinmann S. M., van den Bosch F. C., Yang X., Mo H. J., 2006, *MNRAS*, **366**, 2
- White S. D. M., Rees M. J., 1978, *MNRAS*, **183**, 341
- Wolf C., et al., 2009, *MNRAS*, **393**, 1302
- Yepes G., Kates R., Khokhlov A., Klypin A., 1997, *MNRAS*, **284**, 235
- de Vaucouleurs G., 1961, *ApJS*, **6**, 213
- de Vaucouleurs G., de Vaucouleurs A., Corwin Jr. H. G., Buta R. J., Paturel G., Fouqué P., 1991, *Third Reference Catalogue of Bright Galaxies*. Volume I: Explanations and references. Volume II: Data for galaxies between 0^h and 12^h . Volume III: Data for galaxies between 12^h and 24^h .
- van Gorkom J. H., 2004, *Clusters of Galaxies: Probes of Cosmological Structure and Galaxy Evolution*, p. 305
- van den Bergh S., 1976, *ApJ*, **206**, 883